ACCOUNTS
of chemical research

Quantum Chemistry Behind Bioimaging: Insights from Ab Initio Studies of Fluorescent Proteins and Their Chromophores

KSENIA B. BRAVAYA,[†] BELLA L. GRIGORENKO,[‡] ALEXANDER V. NEMUKHIN,[‡,§] AND ANNA I. KRYLOV*[,†]

[†]*Department of Chemistry, University of Southern California, Los Angeles, California 90089-0482, United States,* [‡]*Department of Chemistry, M.V. Lomonosov Moscow State University, Moscow 119991, Russia, and* [§]*N.M. Emanuel Institute of Biochemical Physics, Russian Academy of Sciences, Moscow 119334, Russia*

RECEIVED ON JUNE 9, 2011

CONSPECTUS

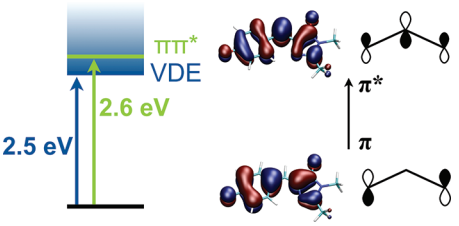

The unique properties of green fluorescent protein (GFP) have been harnessed in a variety of bioimaging techniques, revolutionizing many areas of the life sciences. Molecular-level understanding of the underlying photophysics provides an advantage in the design of new fluorescent proteins (FPs) with improved properties; however, because of its complexity, many aspects of the GFP photocycle remain unknown. In this Account, we discuss computational studies of FPs and their chromophores that provide qualitative insights into mechanistic details of their photocycle and the structural basis for their optical properties. In a reductionist framework, studies of well-defined model systems (such as isolated chromophores) help to understand their intrinsic properties, while calculations including protein matrix and/or solvent demonstrate, on the atomic level, how these properties are modulated by the environment.

An interesting feature of several anionic FP chromophores in the gas phase is their low electron detachment energy. For example, the bright excited $\pi\pi^*$ state of the model GFP chromophore (2.6 eV) lies above the electron detachment continuum (2.5 eV). Thus, the excited state is metastable with respect to electron detachment. This autoionizing character needs to be taken into account in interpreting gas-phase measurements and is very difficult to describe computationally. Solvation (and even microsolvation by a single water molecule) stabilizes the anionic states enough such that the resonance excited state becomes bound. However, even in stabilizing environments (such as protein or solution), the anionic chromophores have relatively low oxidation potentials and can act as light-induced electron donors.

Protein appears to affect excitation energies very little (<0.1 eV), but alters ionization or electron detachment energies by several electron volts. Solvents (especially polar ones) have a pronounced effect on the chromophore's electronic states; for example, the absorption wavelength changes considerably, the ground-state barrier for cis−trans isomerization is reduced, and fluorescence quantum yield drops dramatically. Calculations reveal that these effects can be explained in terms of electrostatic interactions and polarization, as well as specific interactions such as hydrogen bonding.

The availability of efficient computer implementations of predictive electronic structure methods is essential. Important challenges include developing faster codes (to enable better equilibrium sampling and excited-state dynamics modeling), creating algorithms for properties calculations (such as nonlinear optical properties), extending standard excited-state methods to autoionizing (resonance) states, and developing accurate QM/MM schemes.

The results of sophisticated first-principle calculations can be interpreted in terms of simpler, qualitative molecular orbital models to explain general trends. In particular, an essential feature of the anionic GFP chromophore is an almost perfect resonance (mesomeric) interaction between two Lewis structures, giving rise to charge delocalization, bond-order scrambling, and, most importantly, allylic frontier molecular orbitals spanning the methine bridge. We demonstrate that a three-center Hückel-like model provides a useful framework for understanding properties of FPs. It can explain changes in absorption wavelength upon protonation or other structural modifications of the chromophore, the magnitude of transition dipole moment, barriers to isomerization, and even non-Condon effects in one- and two-photon absorption.

Published on the Web 09/01/2011 www.pubs.acs.org/accounts
10.1021/ar2001556

1. Introduction

The unique properties of green fluorescent protein (GFP) exploited in novel bioimaging techniques have revolutionized many areas in life sciences[1,2] and motivated numerous experimental and theoretical studies.[3−9] Owing to the complexity of the system, many aspects of the GFP photocycle and chromophore formation are still unknown. Molecular-level understanding of these processes provides a crucial advantage in the design of new fluorescent proteins (FPs) with improved properties such as better optical output, faster maturation rates, smaller phototoxicity, better spectral separation for FRET pairs, pH or redox sensitive fluorescence, as well as sensitivity to small molecules or ions such as Ca^{2+} or Cl^-. The knowledge of structure−function relationship can also guide the development of new applications of FPs, such as optical highlighting,[5,10] genetically encoded photosensitizers for chromophore-assisted light inactivation (e.g., for photodynamic cancer treatment),[11] and as photochemically active partners.[12]

Numerous excellent reviews highlighted different aspects of GFP chemistry and photophysics and emphasized the synergy between complementary experimental and theoretical approaches.[1,3−7,9] Indeed, no single technique can provide a comprehensive mechanistic picture for a system of such complexity. For example, excited-state proton transfer (ESPT) and recovery of the resting A-form in wt-GFP (wild-type) have been interrogated by ultrafast time-resolved fluorescence experiments, transient vibrational spectroscopy, crystallography, and mutagenesis as well as computational modeling.[4,6] Mechanistic details of red chromophore maturation have been studied by means of X-ray structural analysis, trapped intermediates, kinetic isotope effect, monitoring peroxide production, mass spectrometry, and targeted mutations.[13]

The focus of this Account is on the unique role of theory in studies of FPs. Starting from the first applications of quantum chemistry methods,[14] computational modeling has been used to test structural assumptions, for example, whether the hypothesized structure of a chromophore absorbs at the observed wavelength or to quantify the effect of changes in local environment, protonation state, and so forth on the spectral properties. Calculations of reaction energy profiles can help to discriminate between different maturation mechanisms and proposed intermediates. Exploration of excited-state surfaces and dynamics has contributed toward elucidation of mechanisms of ESPT and radiationless relaxation. Numerous contributions of theory to FP studies have been discussed in refs 4, 6, and 9. In this Account, we highlight qualitative insights into the electronic structure of FP based on the recent work from our laboratories. We also emphasize similarities between the GFP-type chromophores and the chromophore from photoactive (but not fluorescent) yellow protein (PYP).

2. Resonance Interactions and Molecular Orbital Framework

The chromophore of the wt and many other FPs consists of phenolate and imidazolinone moieties connected by a methine bridge. Figure 1 shows chemical structures of the model chromophore, 4-hydroxybenzylidene-2,3-dimethylimidazolinone (HBDI). In the ground state, there is an equilibrium between the protonated and deprotonated (anionic) forms, and their ratio depends on the local environment. For example, in wt-GFP, the chromophore is predominantly protonated, whereas the so-called enhanced GFP (EGFP) features anionic chromophore.

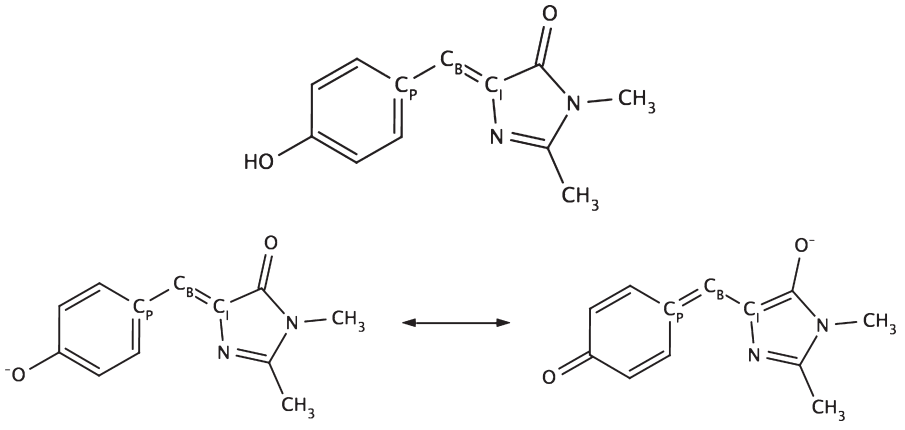

FIGURE 1. Chemical structures and atomic labels of HBDI (top) and deprotonated HBDI (HBDI anion, bottom) in the cis-conformation. The anion's structure is derived from the two interacting resonance structures characterized by different bond orders and charge distribution. The two CH_3 groups represent the covalent bonds by which the chromophore is bound to the protein barrel.

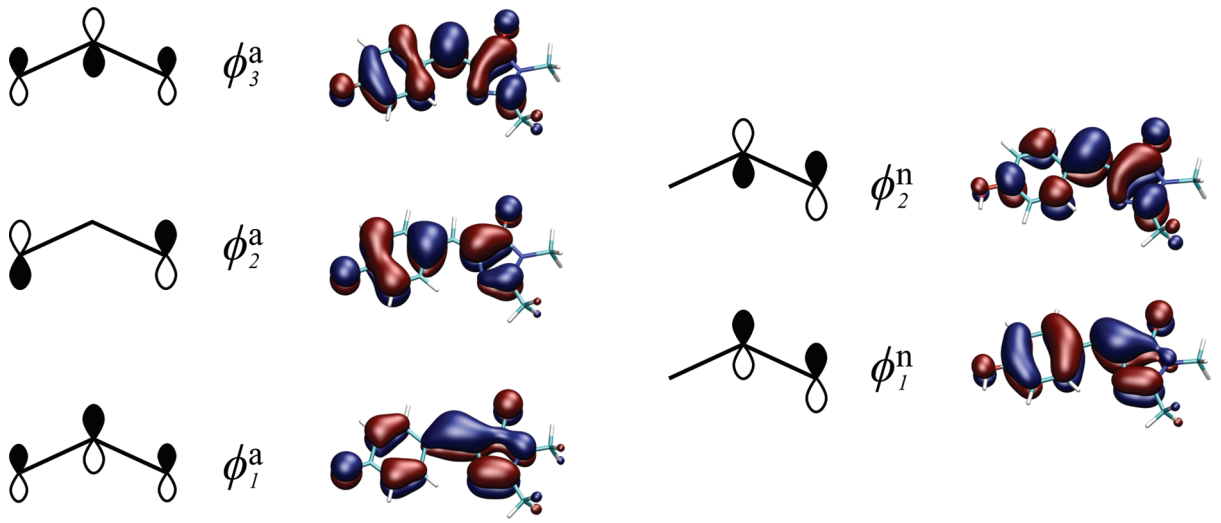

FIGURE 2. Relevant molecular orbitals of deprotonated (left) and neutral (right) HBDI, HF/6-311G(d), and the corresponding solutions of the Hückel model. In the ground state of the anion, both ϕ_1^a and ϕ_2^a are doubly occupied, and the bright state is derived by the $\phi_2^a \rightarrow \phi_3^a$ excitation. In the protonated form (neutral HBDI), the MOs are no longer of allylic character, and the bright excited state resembles a simple ethylene-like $\phi_1^n \rightarrow \phi_2^n$ transition.

The electronic excitation in the protein leads to the ultrafast (sub-picosecond) ESPT producing electronically excited anionic form, which is ultimately responsible for the fluorescence.[1,4,15]

An essential feature of the anionic GFP chromophore is almost a perfect resonance (mesomeric) interaction between the two Lewis structures (see Figure 1). The resonance leads to charge delocalization over the phenolate and imidazolinone moieties and bond-order scrambling, which is clearly reflected by the equilibrium structure.[16] For example, the bridge CC bond lengths (computed by resolution-of-identity second order Møller–Plesset theory, RI-MP2, and cc-pVTZ) are 1.384 Å (C_BC_P) and 1.378 Å (C_BC_I), which can be compared with the typical double and single CC bond lengths of 1.333 and 1.470 Å, respectively.[17] Protonation detunes the resonance stabilizing the phenolate form, which results in more pronounced bond alternation, 1.435 Å (phenolate) and 1.350 Å (imidazolinone),[18] which has consequences for excited-state dynamics.[18–20]

A similar structural motif is observed in the PYP chromophore, where the degree of resonance stabilization varies in different isomers and protonation forms, and is most pronounced in the phenolate form of para-coumaric acid (pCA).[21] The resonance can also be affected by structural modifications, for example, it disappears in the meta-hydroxy isomers of HBDI and pCA.[22,23]

In addition to its effect on the structure and charge distribution, the degree of resonance interaction affects the electronic properties, which can be rationalized within a simple Hückel-like model.[16,18,21,24,25] Similar valence-bond-like models have been employed to explain changes in the absorption wavelengths upon substitutions in dyes[26] and excited-state isomerization of GFP.[27,28]

Figure 2 shows frontier molecular orbitals (MOs) of the anionic (deprotonated) and neutral HBDI. Nearly perfect resonance in the anionic form results in the allylic-type MOs spanning the bridge region (C_P, C_B, and C_I), whereas stabilization of the phenolate moiety by protonation leads to an ethylene-like pattern. Even though the MOs are delocalized over the entire molecule, the electronic density redistribution upon electronic excitation mainly involves the bridge region. Thus, our analysis is based on a model system consisting of the three bridge carbons.

Assuming perfect resonance for the anionic form, the three atoms (C_P, C_B, and C_I) are equivalent and the Hückel Hamiltonian is:

$$H = \begin{pmatrix} \varepsilon & \alpha & 0 \\ \alpha & \varepsilon & \alpha \\ 0 & \alpha & \varepsilon \end{pmatrix} \quad (1)$$

where ε is an atomic *p*-orbital energy and α is a coupling matrix element between the two neighboring centers ($\alpha < 0$). This Hamiltonian is identical to the Hückel's description of the allyl radical; however, the number of electrons is different (four in HBDI versus three in allyl). The diagonalization of this matrix yields the following eigenvalues:

$$E_1^a = \varepsilon + \sqrt{2}\alpha \quad (2)$$

$$E_2^a = \varepsilon \quad (3)$$

$$E_3^a = \varepsilon - \sqrt{2}\alpha \quad (4)$$

The corresponding eigenfunctions $\{\phi_i^a\}_{i=1-3}$ are:

$$\phi_1^a = \frac{1}{2}(p_P + \sqrt{2}p_B + p_I) \quad (5)$$

$$\phi_2^a = \frac{1}{\sqrt{2}}(p_I - p_P) \quad (6)$$

$$\phi_3^a = \frac{1}{2}(p_P - \sqrt{2}p_B + p_I) \quad (7)$$

where p_P, p_B, and p_I are the p-orbitals of the three carbon atoms, C_P, C_B, and C_I, respectively. The eigenfunctions are depicted in Figure 2, next to the respective Hartree–Fock MOs. Indeed, the shapes of the HOMO-1, HOMO, and LUMO in the bridge region are similar to the $\{\phi_i^a\}_{i=1-3}$ Hückel solutions. The HOMO–LUMO ($\phi_2^a \rightarrow \phi_3^a$) excitation energy is $\sqrt{2}|\alpha|$.

In the protonated form, the three carbons are no longer equivalent. Assuming $\varepsilon_P \ll \varepsilon_B = \varepsilon_I = \varepsilon$ and neglecting the coupling between C_P and C_B, we arrive to the following Hamiltonian:

$$h = \begin{pmatrix} \varepsilon' & 0 & 0 \\ 0 & \varepsilon & \alpha \\ 0 & \alpha & \varepsilon \end{pmatrix} \quad (8)$$

which gives rise to the eigenvalues:

$$E_1^n = \varepsilon + \alpha \quad (9)$$

$$E_2^n = \varepsilon - \alpha \quad (10)$$

And the eigenstates are:

$$\phi_1^n = \frac{1}{\sqrt{2}}(p_B + p_I) \quad (11)$$

$$\phi_2^n = \frac{1}{\sqrt{2}}(p_I - p_B) \quad (12)$$

The resulting HOMO–LUMO excitation energy is $2|\alpha|$.

Thus, the model predicts lower excitation energies in the deprotonated form, which is indeed supported by the calculations and the experiment. For example, vertical excitation energies of the anionic and protonated forms are 2.62 and 3.83 eV, respectively [computed by the scaled-opposite-spin configuration interaction singles (CIS) with perturbative account of double excitations method, SOS-CIS(D), and cc-pVTZ; see ref 18]. Likewise, detuned resonance in meta-form of anionic HBDI and pCA results in higher excitation energies.[22,23] A similar trend is observed in the two isomers of anionic pCA: the excitation energy of the carboxylate form is almost 1 eV higher than that of the phenolate form.[21]

This model can also be used to analyze the trends in oscillator strengths (similar to the analysis of Dewar and Longuet-Higgins[29]). For a linear arrangement of the atoms, such that p_B is located at $x = 0$, p_P at $x = -x_0$, p_I at $x = x_0$, that is, $\langle p_B|x|p_B\rangle = 0$, $\langle p_P|x|p_P\rangle = -x_0$, $\langle p_I|x|p_I\rangle = x_0$, and assuming zero overlap between the orbitals centered on different atoms ($\langle p_P|x|p_B\rangle = \langle p_P|x|p_I\rangle = \langle p_B|x|p_I\rangle = 0$), the transition dipole moment matrix element for the anionic form corresponding to the first excitation (HOMO → LUMO) is:

$$\begin{aligned}\langle\phi_2^a|x|\phi_3^a\rangle &= \frac{1}{2\sqrt{2}}\langle -p_P + p_I|x|p_P - \sqrt{2}p_B + p_I\rangle \\ &\approx -\frac{1}{2\sqrt{2}}\langle p_P|x|p_P\rangle + \frac{1}{2\sqrt{2}}\langle p_I|x|p_I\rangle \\ &= \frac{1}{\sqrt{2}}x_0 \end{aligned} \quad (13)$$

and in the neutral (protonated) form:

$$\begin{aligned}\langle\phi_1^n|x|\phi_2^n\rangle &= \frac{1}{2}\langle p_B + p_I|x|p_I - p_B\rangle \\ &\approx \frac{1}{2}\langle p_I|x|p_I\rangle - \frac{1}{2}\langle p_B|x|p_B\rangle = \frac{1}{2}x_0 \end{aligned} \quad (14)$$

Thus, the first excited state ($\pi \rightarrow \pi^*$) in the two forms corresponds to the $\phi_2^a \rightarrow \phi_3^a$ and $\phi_1^n \rightarrow \phi_2^n$ transitions giving rise to the following values of the transition dipole moments: $|\langle\phi_2^a|x|\phi_3^a\rangle|^2 = {x_0}^2/2$ and $|\langle\phi_1^n|x|\phi_2^n\rangle|^2 = {x_0}^2/4$.

Indeed, the computed[18] transition dipole moments of anionic and neutral HBDI (4.05 and 3.18 au) are in qualitative agreement with this prediction. The two pCA^- isomers exhibit a similar trend, although in this case the difference in the computed oscillator strengths is much higher (30 times).[21]

The Hückel model also predicts the trends in excited state energies and oscillator strength of the oxidized species (e.g., electron-detached and doubly electron-detached deprotonated HBDI).[25] In the doublet radical, the excited states are derived from the out-of-phase and in-phase combinations of the $\pi_2 \rightarrow \pi^*$ and $\pi_2 \rightarrow \pi_1$ transitions. Because the respective dipole moment matrix elements have the same magnitude, one of the states is expected to be dark, whereas the second should be bright, which is confirmed by the computed values of the oscillator strengths for D_1 and D_2 (0 and 1.04, respectively).

The above Hückel treatment predicts that all three bright transitions have the same $\langle\mu_{tr}\rangle$. The computed values (CIS/cc-pVTZ) of $|\langle\mu_{tr}\rangle|$ are indeed very close and equal 4.05, 3.74, and 3.75 au for the anion, radical, and cation transitions, respectively. The corresponding values of x_0 (2.8–3.03 Å)

are larger than the CC bond length (1.4 Å), indicating a degree to which the real MOs differ from their simplified allylic representation (Figure 2).

Equation 13 predicts that the oscillator strength of the bright transition will be sensitive to the bridge deformation. For example, CC-bond elongation in the excited state leads to the increased oscillator strength causing preferential enhancement of the corresponding vibrational transitions. This gives rise to non-Condon effects in one and two-photon transitions, as described in section 4.

Finally, the model predicts that the change in the dipole moment upon excitation, $\Delta\mu = \mu_{gr} - \mu_{ex}$, is small. For perfectly allylic orbitals, eqs 5−7, the only nonzero component of the dipole moment (both μ_{gr} and μ_{ex}) is perpendicular to the molecular axis and vanishes at linear geometries. Thus, simple trigonometry predicts small $\Delta\mu$, which is indeed observed in calculations;[16] the computed $|\Delta\mu|$ is 0.6 D, and its direction is in the molecular plain pointing toward the bridge carbon. This value, which is very robust and persists at different levels of theory,[16,30,31] is 10 times smaller than $\Delta\mu$ derived from the Stark effect measurements.[15,32] A possible reason is polarization by the environment, which is supported by the calculations including solvent effects.[30]

3. Electronic Properties of the GFP Chromophore: From Gas Phase to the Protein

Following the so-called reductionist approach, one can attempt to analyze properties of a real complex system from bottom up, that is, from understanding the intrinsic properties of isolated FP chromophores to their behavior in the protein environment. Below we analyze essential features of the anionic FP chromophores in the gas phase and in the protein binding pocket focusing on the interplay between electronically excited states, which give rise to absorption and fluorescence, and ionized (or, more precisely, electron-detached) states responsible for their redox properties.

3.1. Metastable Character of the Excited States in the Anionic GFP Chromophore in the Gas Phase. A characteristic feature of the gas-phase anionic species is relatively low electron detachment energies (DE, energy required to remove an electron). For example, vertical DE (VDE) of the deprotonated HBDI is 2.5 eV.[16,25] VDEs of the two isomers of pCA^- are 2.92 and 3.91 (phenolate and carboxylate form, respectively, ref 21). Thus, the lowest bright excited state in these species lies above the electron-detachment threshold and is, therefore, embedded in the continuum. This makes

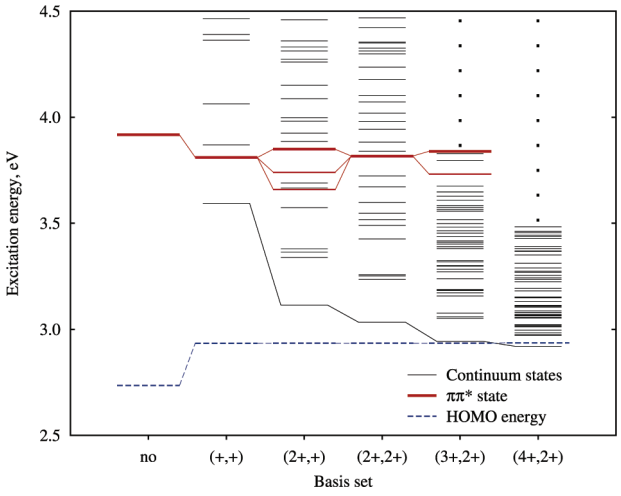

FIGURE 3. Effect of increasing the number of diffuse functions in the basis set on the density of states and convergence of the lowest excited and the bright $\pi\pi^*$ state. The calculations were performed with CIS, and the basis was varied from 6-311G(2pd,2df) to 6-311(4+,2+)G(2pd,2df).

these states metastable with respect to electron detachment, which has implications for the interpretation of the gas-phase experiments.[33−35] Such resonance states have finite lifetime leading to spectral line broadening, and the autoionization channel needs to be properly accounted for in the action spectroscopy experiments. Interestingly, the lowest triplet state that has the same orbital character is below the detachment continuum and is, therefore, a stable bound state.

The resonance character of the excited states has significant consequences for electronic structure calculations, as illustrated in Figure 3. In a small basis set, the excited state appears as an isolated state and its resonance character is only revealed by comparing the excitation energy with the VDE. As the one-electron basis set is expanded, the states approximating the electron-detached continuum start to appear in excited state calculations approaching a well-defined limit, that is, Koopmans VDE in time-dependent DFT (TDDFT) or CIS calculations, or an equation-of-motion (EOM) coupled-cluster with singles and doubles (CCSD) for ionization potentials, EOM-IP-CCSD, value in the EOM-EE-CCSD (EOM-CCSD for excitation energies) calculations. These pseudocontinuum states characterized by increasingly diffuse wave functions and zero oscillator strengths mix with the bright state, making the assignment ambiguous and also causing numeric problems (too many states below the bright state in Davidson diagonalization procedure). Thus, using standard ab initio methods, one cannot reliably calculate the converged (with respect to the basis set) excitation energy of

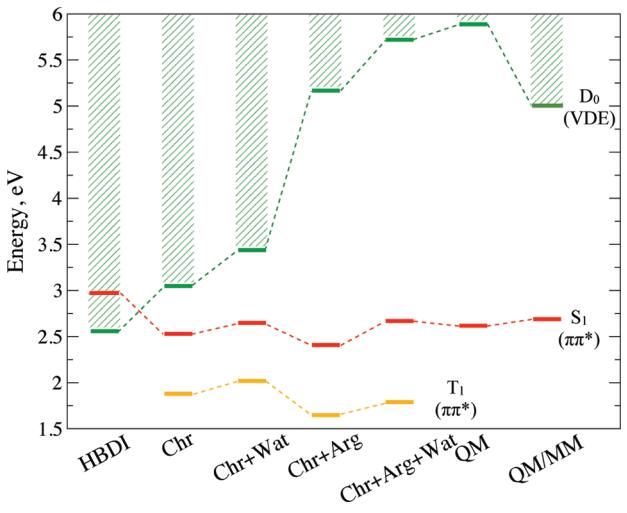

FIGURE 4. Energy diagram of the relevant electronic states of bare HBDI and the GFP chromophore (Chr) in different environments. The complete QM system includes the chromophore, the side chains of Glu222, Arg96 and Ser205, His148, as well as two water molecules, whereas the rest of the protein, solvating water molecules, and counterions are described by MM. See ref 37 for details.

the resonance state (and its spectral broadening due to the interaction with the continuum). Small basis set calculations, which artificially stabilize the resonance, provide only a semiquantitative estimates and need to be carefully analyzed to avoid artifacts due to the interaction with the continuum.[21] In order to address these issues, the extension of standard approaches using complex-scaled Hamiltonians or other techniques are necessary.[36]

3.2. The Effect of the Environment on the Ground, Excited, and Ionized States. Polar environment stabilizes the ground (and excited) state of anions increasing their VDEs. Thus, one can expect that in a solvent or protein environment the excited states of the anionic chromophores would become bound, owing to the VDE increase.

This is indeed confirmed by electronic structure calculations.[37] In the protein, the energy of the excited state is almost unchanged; however, the VDE increases from 2.5 eV (gas phase) up to 5.0 eV. The analysis of different interactions between the chromophore and the surrounding residues reveals that positively charged arginine has the largest stabilizing effect; however, the interactions with other residues and water are also important.

Figure 4 shows excitation energies for the bright $\pi\pi^*$ state, the lowest triplet state, and VDE for the HBDI chromophore in the gas phase and in the protein environment as well as in the model QM clusters of increasing size. In the protein, the energy of the $\pi\pi^*$ excited state is almost unchanged; however, the VDE increases up to 5.0 eV. The convergence of VDE to the bulk value is nonuniform. Adding positively charged arginine leads to the most significant change in VDE relative to the bare chromophore (about 3 eV). The cumulative effect of other neighboring residues in the QM part amounts to about 0.5 eV. The inclusion of the rest of the protein leads to the −0.8 eV change in VDE relative to the QM part. Unlike aqueous solutions, the inclusion of the entire protein and water/counterions in QM/MM results in the VDE decrease relative to the QM value. This is because the stabilizing effect of the nearby charged arginine becomes partially screened by the environment. The VDE is also very sensitive to the positions of solvating water molecules and counterions outside the β barrel despite the large size of the system ($R \sim 36$ Å). The magnitude of the observed variations (up to 0.5 eV) suggests that thermal fluctuations may strongly modulate the VDE.

Interestingly, microhydration of anionic HBDI (or pCA^-) by just one water molecule at either end of the chromophore is sufficient to push the continuum above the excited state.[38] For example, in the lowest isomer of the gas-phase monohydrated anionic HBDI (water at the phenolate end), the interaction with water results in 0.04 eV blue shift in the excitation energy, whereas VDE is blue-shifted by 0.36 eV.[37,38] Thus, a single water molecule is sufficient to convert the $\pi\pi^*$ state from the resonance to the bound state.

A remarkably small effect of the protein on the excitation energy[37] agrees with the experimental observations[33−35] and earlier QM/MM calculations employing different methodology,[39] as well a recent QM/MM study of PYP.[40] Gas-phase action spectroscopy studies[33−35] of deprotonated HBDI have reported vertical excitation energy of 2.6 eV, which is very close to the absorption maximum of GFP at 2.54 eV.[1] Even though the effect of the protein on the excitation energy is small, it plays a crucial role in GFP photophysics by changing the shape of potential energy surfaces (PESs), as discussed in section 4.

The effect of polar solvents such as water is more significant; for example, the blue shift of about 0.2 eV has been observed for the anionic form in ethanol.[41] Moreover, due to changes in electronic state character along cis−trans (or more precisely Z−E) isomerization reaction coordinates, solvation has a pronounced effect on the ground-state isomerization barrier of the deprotonated HBDI; for example, the gas-phase value (computed by multireference and DFT methods) is reduced by more than 10 kcal/mol due to solvent stabilization (estimated using polarized continuum and explicit solvent models) of a charge-localized wave function at the transition state (in terms of the Hückel model,

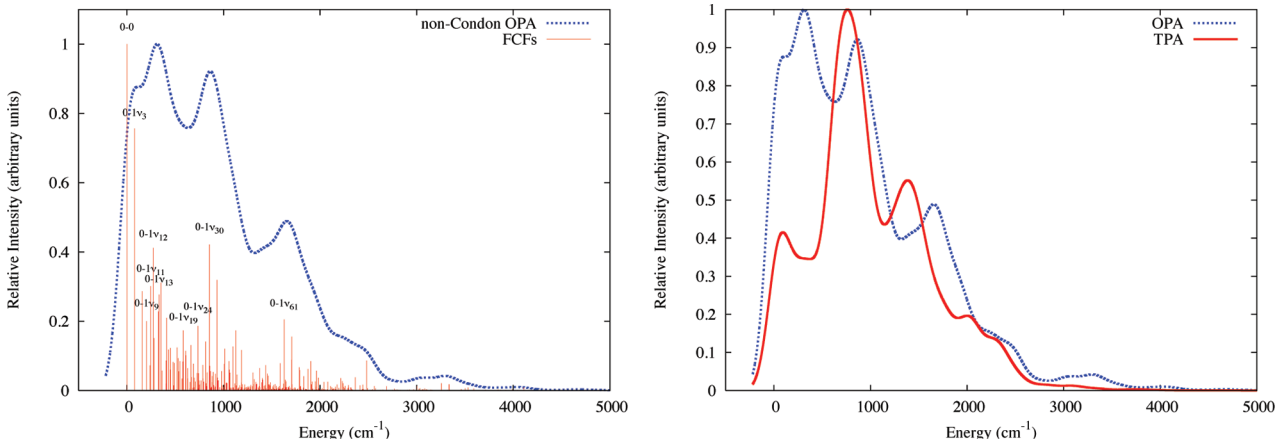

FIGURE 5. Left: FCFs [computed using RI-MP2 and SOS-CIS(D_0) optimized structures] and the OPA spectrum computed within Condon approximation. Right: OPA and TPA spectra computed using vibrational FCFs and including explicit dependence of the transition moments on nuclear geometry (non-Condon effects). See ref 42 for details.

the twisted structure results in the zero overlap between the bridge carbons' p-orbitals, which detunes the resonance leading to charge localization).[24]

4. PES Shapes, Spectroscopy, and Excited-State Dynamics

Photoinitiated dynamics governed by excited-state PES defines the GFP photocycle. Differences in the PES shapes between the ground and excited state give rise to Franck–Condon progressions. Structural relaxation of an electronically excited chromophore, its environment, or ESPT determines Stokes shifts. Most importantly, optical output and brightness are controlled by radiationless relaxation via conical intersections between excited and ground-state PESs.

The MO framework developed in section 2 explains structural changes induced by electronic excitation. In the anionic form, excitation leads to moderate bond-length increase (0.04–0.05 Å) for both bridge CC bonds. The structural relaxation gives rise to several vibrational progressions[42] shown in Figure 5 (top) including bridge deformation modes as well as a variety of ring breathing and bending.

The computed spectrum can be compared with the HBDI action spectrum.[35] As discussed in ref 42, the spectrum based on Franck–Condon factors (FCFs) computed within double-harmonic parallel mode approximation (shown in Figure 5) agrees well with the experimental one at low energies, and is more narrow at higher energies, which could be due to either anharmonic effects (neglected in the simulations) or incomplete deconvolution of the ionization and, especially, autoionization channels in the experiment.

A close inspection of the vibrational spectrum computed by convoluting the corresponding FCFs (see Figure 5) reveals an interesting feature. Note that it is the 0–0 transition and not the vertical one that has the largest individual FCF. However, the higher density of peaks corresponding to combinations of low frequency modes in the region between 300 and 400 cm^{-1} serves to shift the peak of the simulated spectrum. Thus, in large molecules, the peak maximum is likely to be blue-shifted relative to the 0–0 transition and red-shifted relative to vertical electronic energy difference, which should be kept in mind when comparing experimental spectra with electronic structure calculations.

Further changes (a blue shift of 30 cm^{-1} in the peak maximum) in the spectrum are observed when explicit dependence of the transition dipole moment on the nuclear geometry (non-Condon effects) is included. The effect is further enhanced in the two-photon absorption (TPA) cross sections (computed using TDDFT/B3LYP and CIS) owing to their quadratic dependence on transition dipole moments. This results in a blue-shifted TPA spectrum (relative to OPA) by 500 cm^{-1}, which is in excellent agreement with the experimentally reported shift of 700 cm^{-1}.

The structural changes in the neutral HBDI are different;[18] the C_PC_B bond contracts by 0.04 Å, whereas the (formally double) C_BC_I bond elongates by 0.08 Å. The net effect is reduced bond alternation. The energetic relaxation in the excited state is also larger in the neutral form: 21 kcal/mol versus 4 kcal/mol in the anionic form.[18]

These different structural relaxation patterns have consequences for excited state isomerization processes. For example, dynamical simulations[19] demonstrated that the

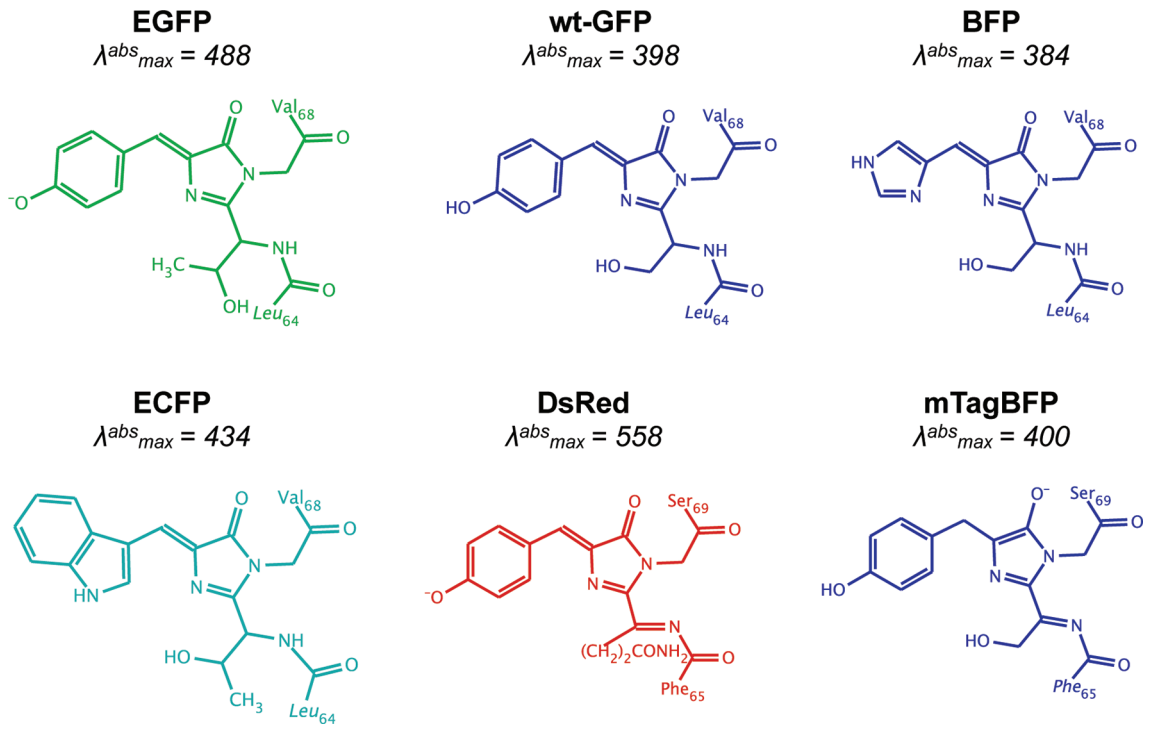

FIGURE 6. Model chromophores representing FPs of different colors: EGFP, wt-GFP, BFP, CFP, DsRed, and TagBFP.

cis−trans isomerization is gated by the protonation state of the phenolate oxygen; in the neutral chromophore, the excited state torsional dynamics involves rotation around the C_BC_I bond, whereas in the anion the rotation around C_BC_P is preferable.

Most importantly, protonation state affects the barrier height separating planar Franck−Condon relaxed structure from conical intersection.[18,43] Whereas the barrier is less than 2 kcal/mol in the anionic chromophore, it is 8−9 kcal/mol in the protonated one. Low barrier in the anionic chromophore is consistent with the observed lack of fluorescence of the isolated chromophore in the gas phase and in solutions. Thus, the role of protein in changing the shapes of the PESs is very important.

5. Controlling the Colors by Structural Modifications of the Chromophore

Imaging applications rely on availability of FPs with specific absorption and emission wavelengths, for example, for color-coding different proteins and cell organelles, devising optimal FRET partners, or pairs of FPs for single excitation-dual emission imaging (which can be achieved by combining two FPs with small and large Stokes shifts). After more than a decade of intense research, the FPs today cover the entire visible spectrum,[2,3] including the red (and far-red) end of the rainbow (absorption/emission above 600 nm or below 2.07 eV), which is of particular importance for mammalian deep tissue imaging.[44]

The colors can be tuned up by changing the chromophore structure or modifying its environment. Let us discuss structural motifs leading to different colors (see Figure 6).

As follows from the Hückel model analysis, lower-energy absorption is achieved by having optimal resonance between the two moieties connected by the allylic bridge. For example, protonation of the anionic HBDI chromophore (as in wt-GFP) or replacing the phenolate ring by His or Trp (as in BFP or ECFP[45]) leads to a blue-shifted absorption relative to anionic HBDI (e.g., in EGFP) that features almost perfect resonance interaction.

Alternatively, as can be rationalized from the particle-in-the-box model, colors can be tuned up by changing the size of the chromophore. For example, most of the red-emitting FPs share the DsRed-like chromophore with the GFP chromophore π-system extended by additional (acylimine) double bond.[46] Reducing the allylic bridge leads to a smaller imidazolinone-acylimine structure characterized by blue/UV absorption.[47−50] Calculations [using SOS-CIS(D) and EOM-CCSD)] predict that, among several possible protonation forms of this blue chromophore, the lowest-energy absorption is observed in the anionic and zwitter-ionic forms that exhibit optimal resonance,[51] whereas protonation of the imidazolinone oxygen leads to 1 eV blue shift.

Recently, a new motif for achieving red-shifted absorption has been proposed.[25] Ab initio calculations have demonstrated that two-electron oxidation of anionic HBDI leads to a positively charged quinoid structure with 0.6 eV red-shifted absorption. The red shift in this cationic structure (proposed as a candidate for the chromophore in oxidative redding[52]) is due to strong stabilization of the virtual orbitals by the positively charged core (thus, it cannot be explained by the Hückel model alone).

6. Conclusions and Outlook

Computer modeling is a powerful tool for understanding and predicting properties of FPs. Quantum chemistry calculations can be used to refine structures, characterize optical properties, compute barriers along reaction coordinates, and more. Most importantly, sophisticated ab initio calculations provide a basis for developing simple qualitative models explaining general trends in electronic structure of FPs.

Using our experience with modeling properties of FP, we would like to highlight strengths and weaknesses of the current quantum chemistry methodology.

An important challenge for theory stems from the size of the system. Even bare chromophores (e.g., HBDI) are quite large for high-level ab initio methods. In QM/MM and QM/EFP approaches that allow one to include the effect of the protein environment, the QM part often includes several neighboring residues, which further increases the cost of the calculations. However, innovative computer codes[53−57] including recent GPU-based implementations[58] enable accurate calculations on a variety of chromophores and chromophores with neighboring residues. For the ground-state properties (structures, frequencies), RI-MP2 and DFT (with appropriate functionals) methods yield reliable results and the calculations are quite fast even with relatively large bases such as cc-pVTZ. In excited-state calculations, the SOS-CIS(D) method (which scales as N^4 when combined with RI) has shown excellent performance; however, the results need to be carefully analyzed, as the approach may fail when the underlying CIS states are nearly degenerate. These situations require methods such as EOM-CCSD, which include both dynamical and nondynamical correlation in one computational step and are particularly suitable for describing interacting states of different character.[59] A number of EOM-CCSD and even CC3 (a CC method that includes perturbative triples correction) calculations have been reported.[16,21,25] Perturbatively corrected multireference calculations have also been performed with quite large active spaces.[39,43,60−62]

An alternative approach is based on carefully parametrized semiempirical models, such as ZINDO.[63] Computational protocols based on DFT/QM/MM geometry optimization and ZINDO/CIS allow one to compute excitation spectra of the FPs for a fraction of the computational time.[64−66]

In addition to energy differences, calculations of other electronic properties are crucial. For example, transition dipole moments are required to discriminate between dark and bright states and to assess which electronic states are accessible spectroscopically. Dipole moments and charge distributions in the ground and excited states help to understand the interaction with the protein environment. For novel applications using nonlinear spectroscopies, properties such as TPA cross sections are needed. While calculations of permanent and transition dipole moments are routine and available for a variety of wave functions, computational tools for nonlinear properties (such as TPA) are relatively scarce.[67]

Finally, the modeling dynamics is often desired to understand lines shapes, Stokes shifts, and fluorescence quantum yield. Several such calculations on complex systems have been reported;[20,68] however, to make dynamics simulations routine, much faster electronic structure codes are needed.

BIOGRAPHICAL INFORMATION

Ksenia B. Bravaya received her M.Sc. (2005) and Ph.D. (2008) in Chemistry from the M.V. Lomonosov Moscow State University, Russia. She is currently a Postdoctoral Research Associate with Prof. Anna I. Krylov at the University of Southern California, Los Angeles. Her posdoctoral work has been recognized by the ACS Physical Chemistry and WISE (USC) Posdoctoral Recognition awards. Dr. Bravaya's major research focus is on theoretical studies of photochemical processes in biomolecules.

Bella Grigorenko received her Ph.D. at the Physics Department of the M.V. Lomonosov Moscow State University in the field of Solid State Physics. Her Doctoral degree (2004) is from the Department of Chemistry at the Moscow State University, where she is currently a Senior Scientist at the Laboratory of Chemical Cybernetics. Dr. Grigorenko's main interests are the development and application of molecular modeling methods to study biomolecular systems.

Alexander Nemukhin is currently Professor of Physical Chemistry at the Chemistry Department of the M.V. Lomonosov Moscow State University and Director of Laboratory for Computer Modeling of Biomolecules and Nanomaterials at the N.M. Emanuel Institute of Biochemical Physics of Russian Academy of Sciences. He received his Ph.D. in 1975 and Doctoral degree in 1989. The theses were devoted to quantum-chemical studies of molecular properties and included collaboration with Professor Jan Almlöf (University of Oslo,

Norway and Minnesota State University) and Professor Frank Weinhold (University of Wisconsin Madison). A substantial part of his early work was devoted to modeling properties of matrix-isolated species at low temperatures. Since 2000, his main research interest is development and application of molecular-modeling methods to study biomolecular systems. He has over 200 publications.

Anna I. Krylov received her M. Sc. (with honors) in Chemistry from the Moscow State University (Russia) in 1990 and her Ph.D. (cum laude) in Physical Chemistry from the Hebrew University of Jerusalem in 1996. After postdoctoral training in Prof. M. Head-Gordon's group at UC Berkeley, she started her research in electronic structure theory and methodology at the Department of Chemistry at the University of Southern California, where she is currently Professor of Chemistry. The focus of her research is on open-shell and electronically excited species ranging from small gas-phase radicals and diradicals relevant to combustion and atmospheric chemistry to biological systems such as ionized DNA and photoactive proteins. Her contributions to electronic structure method development (in particular, Spin-Flip method) have been recognized by several awards including the Dirac medal (2007).

This work was conducted under the auspices of the iOpenShell Center for Computational Studies of Electronic Structure and Spectroscopy of Open-Shell and Electronically Excited Species (http://iopenshell.usc.edu) supported by the National Science Foundation through the CRIF:CRF CHE-0625419+0624602+0625237 grant, as well as through the CHE-0951634 grant (A.I.K.). This work is also supported by the joint grant from the U.S. Civilian Research and Development Foundation (project RUC1-2914-MO-07) and the Russian Foundation for Basic Research (project 10-03-0085).

FOOTNOTES

*To whom correspondence should be addressed.

REFERENCES

1 Tsien, R. Y. The green fluorescent protein. *Annu. Rev. Biochem.* **1998**, *67*, 509–544.

2 Day, R. N.; Davidson, M. W. The fluorescent protein pallete: tools for cellular imaging. *Chem. Soc. Rev.* **2009**, *38*, 2887–2921.

3 Zimmer, M. Green fluorescent protein (GFP): Applications, structure, and related photophysical behavior. *Chem. Rev.* **2002**, *102*, 759–781.

4 Meech, S. R. Excited state reactions in fluorescent proteins. *Chem. Soc. Rev.* **2009**, *38*, 2922–2934.

5 Sample, V.; Newman, R. H.; Zhang, J. The structure and function of fluorescent proteins. *Chem. Soc. Rev.* **2009**, *38*, 2852–2864.

6 van Thor, J. J. Photoreactions and dynamics of the green fluorecent protein. *Chem. Soc. Rev.* **2009**, *38*, 2935–2950.

7 Wachter, R. M. The family of GFP-like proteins: Structure, function, photophysics, and biosensor applications. *Photochem. Photobiol.* **2006**, *82*, 339–344.

8 Tolbert, L. M. ; Baldridge, A. ; Kowalik, J. ; Solntsev, K. M. Collapse and recovery of green fluorescent protein chromophore emission through topological effects. *Acc. Chem. Res.* 2011, published online August 24, http://dx.doi.org/10.1021/ar2000925.

9 Nemukhin, A. V.; Grigorenko, B. L.; Savitskii, A. P. Computer modeling of the structure and spectra of fluorescent proteins. *Acta Nat.* **2009**, *2*, 41–52.

10 Lukyanov, K. A.; Chudakov, D. M.; Lukyanov, S.; Verkhusha, V. V. Photoactivatable fluorescent proteins. *Nat. Rev.* **2005**, *6*, 885–891.

11 Bulina, M. E.; Lukyanov, K. A.; Britanova, O. V.; Onichtchouk, D.; Lukyanov, S.; Chudakov, D. M. Chromophore-assisted light inactivation (CALI) using the phototoxic fluorescent protein KillerRed. *Nat. Protoc.* **2006**, *1*, 947–953.

12 Lukyanov, K. A.; Serebrovskaya, E. O.; Lukyanov, S.; Chudakov, D. M. Fluorescent proteins as light-inducible photochemical partners. *Photochem. Photobiol. Sci.* **2010**, *9*, 1301–1306.

13 Wachter, R. M.; Watkins, J. L.; Kim, H. Mechanistic diversity of red fluorescence acquisition by GFP-like proteins. *Biochemistry* **2010**, *49*, 7417–7427.

14 Voityuk, A. A.; Michel-Beyerle, M.-E.; Rösch, N. Protonation effects on the chromophore of green fluorescent protein. Quantum chemical study of the absorption spectrum. *Chem. Phys. Lett.* **1997**, *272*, 162.

15 Chattoraj, M.; King, B. A.; Bublitz, G. U.; Boxer, S. G. Ultra-fast excited state dynamics in green fluorescent protein: Multiple states and proton transfer. *Proc. Nat. Acad. Sci. U.S.A.* **1996**, *93*, 8362–8367.

16 Epifanovsky, E.; Polyakov, I.; Grigorenko, B. L.; Nemukhin, A. V.; Krylov, A. I. Quantum chemical benchmark studies of the electronic properties of the green fluorescent protein chromophore: I. Electronically excited and ionized states of the anionic chromophore in the gas phase. *J. Chem. Theory Comput.* **2009**, *5*, 1895–1906.

17 Slipchenko, L. V.; Krylov, A. I. Electronic structure of the trimethylenemethane diradical in its ground and electronically excited states: Bonding, equilibrium structures and vibrational frequencies. *J. Chem. Phys.* **2003**, *118*, 6874–6883.

18 Polyakov, I.; Grigorenko, B. L.; Epifanovsky, E.; Grigorenko, B. L.; Krylov, A. I.; Nemukhin, A. V. Potential energy landscape of the electronic states of the GFP chromophore in different protonation forms: Electronic transition energies and conical intersections. *J. Chem. Theory Comput.* **2010**, *6*, 2377–2387.

19 Olsen, S.; Lamothe, K.; Martinez, T. J. Protonic gating of excited-state twisting and charge localization in GFP chromophores: A mechanistic hypothesis for reversible photoswitching. *J. Am. Chem. Soc.* **2010**, *132*, 1192–1193.

20 Virshup, A. M.; Punwong, C.; Pogorelov, T. V.; Lindquist, B. A.; Ko, C.; Martinez, T. J. Photodynamics in complex environments: Ab initio multiple spawning quantum mechanical/molecular mechanical dynamics. *J. Phys. Chem. B* **2009**, *113*, 3280–3291.

21 Zuev, D.; Bravaya, K. B.; Crawford, T. D.; Lindh, R.; Krylov, A. I. Electronic structure of the two isomers of the anionic form of p-coumaric acid chromophore. *J. Chem. Phys.* **2011**, *134*, 034310.

22 Solntsev, K. M.; Poizat, O.; Dong, J.; Rehault, J.; Lou, Y.; Burda, C.; Tolbert, L. M. Meta and para effects in the ultrafast excited-state dynamics of the green fluorescent protein chromophores. *J. Phys. Chem. B* **2008**, *112*, 2700–2711.

23 Rocha-Rinza, T.; Christiansen, O.; Rahbek, D. B.; Klaerke, B.; Andersen, L. H.; Lincke, K.; Nielsen, M. B. Spectroscopic implications of the electron donor-acceptor effect in the photoactive yellow protein chromophore. *Chem.—Eur. J.* **2010**, *16*, 11977–11984.

24 Polyakov, I.; Epifanovsky, E.; Grigorenko, B. L.; Krylov, A. I.; Nemukhin, A. V. Quantum chemical benchmark studies of the electronic properties of the green fluorescent protein chromophore: II. Cis-trans isomerization in water. *J. Chem. Theory Comput.* **2009**, *5*, 1907–1914.

25 Epifanovsky, E.; Polyakov, I.; Grigorenko, B. L.; Nemukhin, A. V.; Krylov, A. I. The effect of oxidation on the electronic structure of the green fluorescent protein chromophore. *J. Chem. Phys.* **2010**, *132*, 115104.

26 Dewar, M. J. S. Colour and constitution. Part I. Basic dyes. *J. Chem. Soc.* **1950**, 2329.

27 Olsen, S.; Smith, S. C. Bond selection in the photoisomerization reaction of anionic green fluorescent protein and kindling fluorescent protein chromophore models. *J. Am. Chem. Soc.* **2008**, *130*, 8677–8689.

28 Olsen, S.; McKenzie, R. H. A diabatic three-state representation of photoisomerisation in the green fluorescent protein chromophore. *J. Chem. Phys.* **2009**, *130*, 184302.

29 Dewar, M. J. S.; Longuet-Higgins, H. C. The electronic spectra of aromatic molecules I: benzenoid hydrocarbons. *Proc. Phys. Soc., London, Sect. A* **1954**, *67*, 795.

30 Yan, W.; Zhang, L.; Xie, D.; Zheng, J. Electronic excitations of green fluorescent proteins: Modeling solvatochromic shifts of red fluorescent protein chromophore model compound in aqueous solutions. *J. Phys. Chem. B* **2007**, *111*, 14055–14063.

31 Das, A. K.; Hasegawa, J.-Y.; Miyahara, T.; Ehara, M.; Nakatsuji, H. Electronic excitations of the green fluorescent protein chromophore in its protonation states: SAC/SAC-CI study. *J. Comput. Chem.* **2003**, *24*, 1421–1431.

32 Bublitz, G.; King, B. A.; Boxer, S. G. Electronic structure of the chromophore in green fluorescent protein (GFP). *J. Am. Chem. Soc.* **1998**, *120*, 9370–9371.

33 Nielsen, S. B.; Lapierre, A.; Andersen, J. U.; Pedersen, U. V.; Tomita, S.; Andersen, L. H. Absorption spectrum of the green fluorescent protein chromophore anion in vacuo. *Phys. Rev. Lett.* **2001**, *87*, 228102.

34 Andersen, L. H.; Lappierre, A.; Nielsen, S. B.; Nielsen, I. B.; Pedersen, S. U.; Pedersen, U. V.; Tomita, S. Chromophores of the green fluorescent protein studied in the gas phase. *Eur. Phys. J. D* **2002**, *20*, 597–600.

35 Forbes, M. W.; Jockusch, R. A. Deactivation pathways of an isolated green fluorescent protein model chromophore studied by electronic action spectroscopy. *J. Am. Chem. Soc.* **2009**, *131*, 17038–17039.

36 Reinhardt, W. P. Complex coordinates in the theory of atomic and molecular structure and dynamics. *Annu. Rev. Phys. Chem.* **1983**, *33*, 223–255.

37 Bravaya, K.; Khrenova, M. G.; Grigorenko, B. L.; Nemukhin, A. V.; Krylov, A. I. The effect of protein environment on electronically excited and ionized states of the green fluorescent protein chromophore. *J. Phys. Chem. B* **2011**, *8*, 8296–8303.

38 Zuev, D.; Bravaya, K.; Makarova, M.; Krylov, A. I. The effect of microhydration on electronically excited and ionized states of model GFP and PYP chromophores. In preparation.

39 Sinicropi, A.; Anduniow, T.; Ferre, N.; Basosi, R.; Olivucci, M. Properties of the emitting state of the green fluorescent protein resolved at the CASPT2//CASSCF/CHARMM level. *J. Am. Chem. Soc.* **2005**, *127*, 11534–11535.

40 Rocha-Rinza, T.; Sneskov, K.; Christiansen, O.; Ryde, U.; Kongsted, J. I. Unraveling the similarity of the photoabsorption of deprotonated p-coumaric acid in the gas phase and within the photoactive yellow protein. *Phys. Chem. Chem. Phys.* **2011**, *13*, 1585–1589.

41 Voityuk, A. A.; Kummer, A. D.; Michel-Beyerle, M. E.; Rösch, N. Absorption spectra of the GFP chromophore in solution: comparison of theoretical and experimental results. *Chem. Phys.* **2001**, *269*, 83–91.

42 Kamarchik, E.; Krylov, A. I. Non-Condon effects in one- and two-photon absorption spectra of the green fluorescent protein. *J. Phys. Chem. Lett.* **2011**, *2*, 488–492.

43 Martin, M. E.; Negri, F.; Olivucci, M. Origin, nature, and fate of the fluorescent state of the green fluorescent protein chromophore at the CASPT2//CASSCF resolution. *J. Am. Chem. Soc.* **2004**, *126*, 5452–5464.

44 Lin, M. Z.; McKeown, M. R.; Ng, H.-L.; Aguilera, T. A.; Shaner, N. C.; Campbell, R. E.; Adams, S. R.; Gross, L. A.; Ma, W.; Alder, T.; Tsien, R. Y. Autofluorescent proteins with excitation in the optical window for intravital imaging in mammals. *Chem. Biol.* **2009**, *16*, 1169–1179.

45 Ai, H. W.; Henderson, J. N.; Remington, S. J.; Campbell, R. E. Directed evolution of a monomeric, bright and photostable version of Clavularia cyan fluorescent protein: structural characterization and applications in fluorescence imaging. *Biochem. J.* **2006**, *400*, 531–540.

46 Gross, L. A.; Baird, G. S.; Hoffman, R. C.; Baldridge, K. K.; Tsien, R. Y. The structure of the chromophore within DsRed, a red fluorescent protein from coral. *Proc. Natl. Acad. Sci. U.S.A.* **2000**, *97*, 11990–11995.

47 Verkhusha, V. V.; Chudakov, D. M.; Gurskaya, N. G.; Lukyanov, S.; Lukyanov, K. A. Common pathway for the red chromophore formation in fluorescent proteins and chromoproteins. *Chem. Biol.* **2004**, *11*, 845–854.

48 Pletnev, S.; Subach, F. V.; Dauter, Z.; Wlodawer, A.; Verkhusha, A. Understanding blue-to-red conversion in monomeric fluorescent timers and hydrolytic degradation of their chromophores. *J. Am. Chem. Soc.* **2010**, *132*, 2243–2253.

49 Subach, F. V.; Malashkevich, V. N.; Zencheck, W. D.; Xiao, H.; Filonov, G. S.; Almo, S. C.; Verkhusha, V. V. Photoactivation mechanism of pamcherry based on crystal structures of the protein in the dark and fluorescent states. *Proc. Natl. Acad. Sci. U.S.A.* **2009**, *106*, 21097–21102.

50 Subach, O. M.; Gundorov, I. S.; Yoshimura, M.; Subach, F. V.; Zhang, J.; Grüenwald, D.; Souslova, E. A.; Chudakov, D. M.; Verkhusha, V. V. Conversion of red fluorescent protein into a bright blue form. *Chem. Biol.* **2008**, *15*, 1116–1124.

51 Bravaya, K. B.; Korovina, N.; Subach, O.; Verkhusha, V. V.; Krylov, A. I. An insight into the common mechanism of the chromophore formation in the red fluorescent proteins: The elusive blue intermediate exposed. *Ang. Chem. Int. Ed.* **2011**, *submitted*.

52 Bogdanov, A. M.; Mishin, A. S.; Yampolsky, I. V.; Belousov, V. V.; Chudakov, D. M.; Subach, F. V.; Verkhusha, V. V.; Lukyanov, S.; Lukyanov, K. A. Green fluorescent proteins are light-induced electron donors. *Nat. Chem. Biol.* **2009**, *5*, 459–461.

53 Shao, Y.; Molnar, L. F.; Jung, Y.; Kussmann, J.; Ochsenfeld, C.; Brown, S.; Gilbert, A. T. B.; Slipchenko, L. V.; Levchenko, S. V.; O'Neil, D. P.; Distasio, R. A., Jr.; Lochan, R. C.; Wang, T.; Beran, G. J. O.; Besley, N. A.; Herbert, J. M.; Lin, C. Y.; Van Voorhis, T.; Chien, S. H.; Sodt, A.; Steele, R. P.; Rassolov, V. A.; Maslen, P.; Korambath, P. P.; Adamson, R. D.; Austin, B.; Baker, J.; Bird, E. F. C.; Daschel, H.; Doerksen, R. J.; Dreuw, A.; Dunietz, B. D.; Dutoi, A. D.; Furlani, T. R.; Gwaltney, S. R.; Heyden, A.; Hirata, S.; Hsu, C.-P.; Kedziora, G. S.; Khalliulin, R. Z.; Klunziger, P.; Lee, A. M.; Liang, W. Z.; Lotan, I.; Nair, N.; Peters, B.; Proynov, E. I.; Pieniazek, P. A.; Rhee, Y. M.; Ritchie, J.; Rosta, E.; Sherrill, C. D.; Simmonett, A. C.; Subotnik, J. E.; Woodcock, H. L., III; Zhang, W.; Bell, A. T.; Chakraborty, A. K.; Chipman, D. M.; Keil, F. J.; Warshel, A.; Herhe, W. J.; Schaefer, H. F., III; Kong, J.; Krylov, A. I.; Gill, P. M. W.; Head-Gordon, M. Advances in methods and algorithms in a modern quantum chemistry program package. *Phys. Chem. Chem. Phys.* **2006**, *8*, 3172–3191.

54 Crawford, T. D.; Sherrill, C. D.; Valeev, E. F.; Fermann, J. T.; King, R. A.; Leininger, M. L.; Brown, S. T.; Janssen, C. L.; Seidl, E. T.; Kenny, J. P.; Allen, W. D. PSI3: An open-source ab initio electronic structure package. *J. Comput. Chem.* **2007**, *28*, 1610–1616.

55 Aquilante, F.; de Vico, L.; Ferré, N. ; G.; Malmqvist, P-Å; Neogrády, P.; Pedersen, T. B.; Piton)k, M.; Reiher, M.; Roos, B.; Serrano-Andrés, L.; Urban, M.; Veryazov, V.; Lindh, R. Molcas 7: The next generation. *J. Comput. Chem.* **2010**, *31*, 224–247.

56 Schmidt, M. W.; Baldridge, K. K.; Boatz, J. A.; Elbert, S. T.; Gordon, M. S.; Jensen, J. H.; Koseki, S.; Mastunaga, N.; Nguyen, K. A.; Su, S.; Windus, T. L.; Dupuis, M.; Montgomery, J. A. General atomic and molecular electronic structure system. *J. Comput. Chem.* **1993**, *14*, 1347–1363.

57 Granovsky, A. A. *PC GAMESS/Firefly*; http://classic.chem.msu.su/gran/gamess.

58 Isborn, C. M.; Luehr, N.; Ufimtsev, I. S.; Martinez, T. J. Excited-state electronic structure with configuration interaction singles and Tamm-Dancoff time-dependent density functional theory on graphical processing units. *J. Chem. Theory Comput.* **2011**, *7*, 1814–1823.

59 Krylov, A. I. Equation-of-motion coupled-cluster methods for open-shell and electronically excited species: The hitchhiker's guide to Fock space. *Annu. Rev. Phys. Chem.* **2008**, *59*, 433–462.

60 Andersen, L. H.; Bochenkova, A. V. The photophysics of isolated protein chromophores. *Eur. Phys. J. D* **2009**, *51*, 5–14.

61 Bravaya, K. B.; Bochenkova, A. V.; Granovsky, A. A.; Savitsky, A. P.; Nemukhin, A. V. Modeling photoabsorption of the asFP595 chromophore. *J. Phys. Chem. A* **2008**, *112*, 8804–8810.

62 Altoé, P.; Bernardi, F.; Garavelli, M.; Orlandi, G.; Negri, F. Solvent effects on the vibrational activity and photodynamics of the green fluorescent protein chromophore: A quantum-chemical study. *J. Am. Chem. Soc.* **2005**, *127*, 3952–3963.

63 Zerner, M. C. Reviews in Computational Chemistry, Volume 2. Lipkowitz, K. B., Boyd, D. B., Eds.; VCH Publishing, New York, 1991; pages 313−316.

64 Topol, I. A.; Collins, J.; Polyakov, I.; Grigorenko, B. L.; Nemukhin, A. V. On photoabsorption of the neutral form of the green fluorescent protein chromophore. *Biophys. Chem.* **2009**, *145*, 1–6.

65 Topol, I.; Collins, J.; Nemukhin, A. Modeling spectral tuning in monomeric teal fluorescent protein mTFP1. *Biophys. Chem.* **2010**, *149*, 78–82.

66 Topol, I.; Collins, J.; Savitsky, A.; Nemukhin, A. Computational strategy for tuning spectral properties of red fluorescent proteins. *Biophys. Chem.* **2011**, *158*, 91–95.

67 DALTON, a molecular electronic structure program, Release 2.0. http://www.kjemi.uio.no/software/dalton/dalton.html, 2005.

68 Levine, B. G.; Martinez, T. J. Isomerization through conical intersections. *Annu. Rev. Phys. Chem.* **2007**, *58*, 613–634.